

Complete Mitochondrial Genome of the Steppe Ribbon Racer (*Psammophis lineolatus*): The First Representative from the Snake Family Psammophiidae and its Phylogenetic Implications

Minli CHEN^{1,2}, Jinlong LIU², Jun LI³, Na WU^{1,2} and Xianguang GUO^{1*}

¹ Chengdu Institute of Biology, Chinese Academy of Sciences, Chengdu 610041, Sichuan, China

² University of Chinese Academy of Sciences, Beijing 100049, China

³ College of Life Science and Technology, Xinjiang University, Urumqi 830046, Xinjiang, China

Abstract Comparisons of vertebrate mitochondrial genomes (mitogenomes) may yield significant insights into the evolution of organisms and genomes. However, no complete mitogenome from the snake family Psammophiidae has been reported. In this study, we sequenced and annotated the complete mitogenome of *Psammophis lineolatus*, representing the first mitogenome of Psammophiidae. The total length is 17 166 bp, consisting of 13 protein-coding genes (PCGs), 22 transfer RNAs (tRNAs), two ribosomal RNAs (12S rRNA and 16S rRNA), and duplicate control regions (CRs). This gene arrangement belongs to the Type III pattern, which is a widely shared gene order in Alethinophidian snakes. All tRNAs exhibit cloverleaf structures with the exception of tRNA-Ser^{AGY} and tRNA-Pro, which lack a dihydrouridine (DHU) arm/stem and TΨC loop, respectively. The 13 PCGs include five start codons (ATG, GTG, ATA, ATT, and ATC), two complete stop codons (TAA and AGG), and two incomplete stop codon (T- and TA-). In addition, the Ka/Ks ratios indicate that all PCGs had undergone a strong purifying selection. Four types of CR domains rearrangement occurred among eight species of Elapoidea. The phylogenetic reconstructions with both Bayesian inference and maximum likelihood methods support the placement of Psammophiidae in the Elapoidea superfamily,

with Homalopsidae being the sister taxon to Elapoidea and Colubroidea. However, the sister taxon of Psammophiidae is unclear due to the availability of Elapoidea mitogenomes being limited to the family Elapidae. More mitogenomes from different taxonomic groups in Elapoidea are needed to better understand the phylogenetic relationships within Elapoidea.

Keywords mitochondrial genome, phylogenetic relationships, *Psammophis lineolatus*, Psammophiidae, purifying selection

1. Introduction

During the last four decades, sequences of the mitochondrial genomes (mitogenomes) of thousands of Metazoan species have been produced and are freely available in GenBank (<https://www.ncbi.nlm.nih.gov/genbank/>). Approximately two thirds of these sequences are from vertebrates. These sequences have been successfully applied to phylogenetic analyses at both shallow and deep levels (e.g., Bernt *et al.*, 2013a; Knaus *et al.*, 2011), as well as for analyses of mitogenome organization and evolution (e.g., Bernt *et al.*, 2013b; Boore, 1999; Mauro *et al.*, 2006). As the number of mitogenome sequences continues to increase, it has become clear that, rearrangements of several transfer RNA genes (tRNAs) are quite common (e.g., Mauro *et al.*, 2006; Pereira, 2000; Xia *et al.*, 2016), even though gene arrangement is quite stable across many vertebrates. Overall, most vertebrate mitogenomes contain the same 37 genes (two for rRNAs, 13 for proteins and 22 for tRNAs), but their order is variable among – and to a lesser extent, within – major groups (Bernt

* Corresponding author: Dr. Xianguang GUO, from Chengdu Institute of Biology, Chinese Academy of Sciences, Chengdu, China, with his research focusing on taxonomy, phylogeny and biogeography of amphibians and reptiles in arid Central Asia.

E-mail: guoxg@cib.ac.cn

Received: 9 December 2020 Accepted: 27 March 2021

et al., 2013; Boore, 1999; Pereira, 2000). Accordingly, comparisons of vertebrate mitochondrial genomes may lead to significant insights into the evolution both of organisms and of genomes.

Snakes, which are members of the suborder Serpentes in Squamata, are an example of a group having a dynamic mitogenome structure. Currently, there are over 3700 recognized snake species, comprising two major clades: Scolecophidia (blind snakes) and Alethinophidia (Uetz *et al.*, 2020). Scolecophidia are small fossorial snakes that feed mainly on ants and termites. Alethinophidia includes Henophidia (primitive snakes) and Caenophidia (advanced snakes; including ~80% of extant snakes) (Vidal and Hedges, 2002a). Some unique characteristics have been reported in the mitogenomes of snakes, including duplicate control regions (CRs), gene order rearrangements, shorter tRNA genes, and other shortened genes (Chen and Zhao, 2009; Douglas and Gower, 2010; Jiang *et al.*, 2007). To date, 11 types of rearrangement patterns have been detected in snake mitogenomes (Type I, II, III, III-A, III-B, III-B1, III-C, III-D, III-E, III-F, III-G) (Qian *et al.*, 2018). Among these, Type III is characterized by duplication of the CR and translocation of the tRNA-Leu gene; it is also the most common gene arrangement, extensively distributed in Alethinophidia. These arrangements are thought to involve three main processes: gene loss, translocation and duplication (Qian *et al.*, 2018). Although a few convergent gene rearrangements have been observed in vertebrate mtDNAs, many derived genomic rearrangements are clearly useful as phylogenetic makers (thus, synapomorphic characters) for the identification of monophyletic groups (Boore and Brown, 1998; Okajima and Kumazawa, 2010; Xia *et al.*, 2014). Therefore, mitogenome data will contribute to our phylogenetic understanding of snakes, as well as the evolutionary implications of their mitogenomic rearrangements.

As of October 1, 2020, there were 188 complete mitogenomes of snakes present in the NCBI RefSeq database (Pruitt *et al.*, 2007), covering 124 snake species. However, no complete mitogenome from the family Psammophiidae (formerly the subfamily Psammophiinae; Bourgeois, 1968) has ever been reported. This family comprises a natural group occurring throughout Africa, the Middle East, Madagascar, southern Europe and south-central Asia (Dowling and Duellman, 1978; Kelly *et al.*, 2003; Kelly *et al.*, 2009), and currently consists of eight genera and 55 extant species (Uetz *et al.*, 2020). Many studies of Psammophiidae have focused on systematics based on morphological features (Bourgeois, 1968; Dowling and Duellman, 1978; Zaher, 1999). Although there are some molecular studies, most are based on limited mitochondrial DNA fragments and/or nuclear genes (Gravlun, 2001; Kelly *et al.*, 2008; Kelly *et al.*, 2009; Lawson *et al.*, 2005; Nagy *et al.*, 2003; Vidal and Hedges, 2002b).

In this study, we produced for the first time the complete mitogenome sequence of the Steppe Ribbon Racer, *Psammophis lineolatus* (Brandt, 1838), a representative of the family Psammophiidae. As noted by Qian *et al.* (2018), the Type III mitogenome rearrangement is the most prevalent and widely occurring in Elapidae. Given that Psammophiidae is closely related to Elapidae among the major snake families – both belonging to the Elapoidea superfamily (Figueroa *et al.*, 2016; Kelly *et al.*, 2009; Zaher *et al.*, 2019) – we predict that the mitogenome arrangement of *P. lineolatus* would belong to the Type III pattern. In addition, we used the mitogenome to infer the phylogenetic position of Psammophiidae in the major lineages of the advanced snakes.

2. Materials and Methods

2.1. Sample collection and DNA extraction A *P. lineolatus* specimen was captured by hand in Buerjin County (47.559316°N, 87.056509°E), Xinjiang Uygur Autonomous Region, China in July 2019. A piece of liver was dissected from the snake, which has been euthanized with an overdose of sodium pentobarbital delivered by intraperitoneal injection. Both the liver sample and voucher specimen (Field number GXG311) were fixed in 95% ethanol, and deposited at the herpetological collection, Chengdu Institute of Biology, Chinese Academy of Sciences. Total genomic DNA was extracted using the TIANamp Genomic DNA Kit (TIANGEN, Beijing, China) following the manufacturer's instructions, and stored at –20°C. The amount and quality of the extracted DNA were assessed through electrophoresis in a 0.8% agarose gel with GoldView (Solarbio, Beijing, China).

2.2. PCR amplification and sequencing Twenty pairs of primers (Table S1) were designed to amplify the complete mitogenome, based on published mitogenomes from Elapidae (GenBank accession number: EU579523, GU045453). The polymerase chain reaction (PCR) amplification was carried out in volumes of 25 µL consisting of 2 µL template DNA (~40 ng/µL), 2.5 µL dNTPs (0.2 mmol/L each), 1.5 µL MgSO₄ (1.5 mmol/L), 2.5 µL buffer of KOD-plus neo (TOYOBO, Shanghai, China), 0.5 µL KOD-plus neo (1.0 U/µL), 0.75 µL each primer (0.3 µmol/L), and 14.5 µL ultrapure water. Thermal cycling was performed with an initial denaturation at 94°C for 2 min, followed by 32–35 cycles of 98°C for 10 s, 45–60°C (depending on the primers) for 30 s, and 68°C for 60–90 s; the reaction concluded with a final extension of 7 min at 68°C, then stored at 4°C. The PCR products were assessed using 1% agarose gel electrophoresis, purified, and sequenced with the PCR primers and internal primers generated by primer walking. All fragments were sequenced on an ABI 3730 automated sequencer (Applied Biosystems, Inc.) at TsingKe Biotech (Beijing, China).

2.3. Genome assembly, annotation and analysis

Mitochondrial DNA fragments were assembled to create the complete mitochondrial genome using the SeqMan II program included in the Lasergene software package (DNASTar Inc., Madison, USA). The complete mitogenome was submitted to GenBank using the software of Sequin v15.10 (<http://www.ncbi.nlm.nih.gov/Sequin/>). The boundaries of the protein-coding genes (PCGs) and ribosomal RNA genes (rRNAs) were identified using NCBI-BLAST (<http://blast.ncbi.nlm.nih.gov/>) and MITOS Web Server (<http://mitos2.bioinf.uni-leipzig.de/index.py>) (Bernt *et al.*, 2013c). The tRNAs and their potential cloverleaf structures were predicted using tRNAscan-SE Search Server v1.21 (<http://lowelab.ucsc.edu/tRNAscan-SE/>) (Lowe and Chan, 2016), and verified by aligning them with other snakes. The size of the CR was confirmed by the boundaries of tRNAs and by sequence comparison with previously reported snake mitogenomes. A circular mitogenomic map was generated using OGDRAW v1.3.1 (Greiner *et al.*, 2019). Base composition and the relative synonymous codon usage (RSCU) values were calculated using MEGA v7.0 (Kumar *et al.*, 2016). Strand asymmetry was calculated using the formulae: $AT\text{-skew} = (A - T)/(A + T)$; $GC\text{-skew} = (G - C)/(G + C)$ (Perna and Kocher, 1995).

Ka/Ks is the ratio of the number of nonsynonymous substitutions per nonsynonymous site (Ka) to the number of synonymous substitutions per synonymous site (Ks) (Hurst, 2002). This ratio is considered to be a good indicator of selective pressure at the sequence level (Yang and Bielawski, 2000) and has been used to identify PCGs under positive and purifying selection in a wide range of organisms (Hurst, 2009). In general, positive selection yields a Ka/Ks ratio greater than 1. Conversely, if purifying selection occurs, the Ka/Ks ratio is less than 1, which would lead to a decrease in diversity at the amino acid level. Therefore, to determine the direction of natural selection (positive or purifying) of the PCGs at the molecular level, we calculated the Ka/Ks ratio of each PCG between *P. lineolatus* and three Elapidae snakes (*Bungarus multicinctus*, *Naja naja* and *Ophiophagus Hannah*) using DnaSP v6.12.03 (Rozas *et al.*, 2017).

2.4. Phylogenetic reconstruction Phylogenetic analyses were conducted using the mitochondrial genome (excluding the CR) to infer the placement of Psammophiidae within the advanced snakes (Table S2). Complete gene sequences from representatives of the major snake families were chosen following a recent study (Qian *et al.*, 2018), and were retrieved from GenBank. Each gene was extracted from the whole mitogenome, then separately aligned in batches with MAFFT v7.263 (Katoh and Standley, 2013) using ‘-auto’ strategy and normal alignment mode. In total, 37 mitochondrial genes were combined from 71 taxa using SeaView v5.0.1 (Gouy *et al.*, 2010),

which formed a dataset of 15 838 bp in length. Considering that Henophidia is closely related to Caenophidia (Streicher and Wiens, 2016; Yan *et al.*, 2008), six Henophidia snake species, representing six families, were chosen as outgroup taxa (Table S2). Among these, Tropidophiidae and Aniliidae were used to root the trees based on two recent publications (Qian *et al.*, 2018; Streicher and Wiens, 2016).

Prior to the phylogenetic analyses, optimal combinations of partitioning schemes and nucleotide substitution models were determined with PartitionFinder v2.1.1 (Lanfear *et al.*, 2017), using the “greedy” algorithm and the Akaike information criterion. The branch lengths of alternative partitions were linked and the “mrBayes” model was used to estimate the best substitution model for IQ-TREE and MrBayes. The best-fit substitution models and partitioning schemes for each gene are given in Table S3.

Phylogenetic analyses were performed with Bayesian inference (BI) and maximum likelihood (ML) methods. Bayesian phylogenies were inferred using MrBayes v3.2.6 (Ronquist *et al.*, 2012) under partitioned models. Two independent runs were conducted with four Markov Chain Monte Carlo (MCMC) for 10,000,000 generations with parameters and topologies sampled every 1000 generations. When the average standard deviation of split frequencies reached a value of less than 0.01, the initial 25% trees were discarded as burn-in and the remaining trees were used to calculate Bayesian posterior probabilities (PP). Maximum likelihood analyses were conducted in IQ-TREE v1.6.12 (Nguyen *et al.*, 2015) under the models selected for each identified partition. We assessed nodal support using 5000 bootstrap pseudoreplicates via the ultrafast-bootstrap (UFBoot) (Minh *et al.*, 2013) method. Nodes with UFBoot ≥ 95 were considered to be well-supported (Minh *et al.*, 2013; Wilcox *et al.*, 2002). Finally, the trees were visualized and edited in FigTree v1.4.2 (<http://tree.bio.ed.ac.uk/software/figtree>) and PowerPoint.

3. Results and Discussion

3.1. Genome structure, organization and composition The complete sequence of the mitogenome of *P. lineolatus* (accession number MT991050) is a traditional circular, double-strain DNA molecule (Figure 1). It contains 37 genes with 13 PCGs, two rRNA genes, and 22 tRNA genes but two control regions (CR I, CR II) (Table 1). However, the tRNA-Leu^{UUR} (Leu2) gene was translocated; in most vertebrates, it is between 16S rRNA and NDI, but in snakes it is between tRNA-Ile and tRNA-Gln (Figure 1). The gene order is in agreement with the Type III pattern designated by Qian *et al.* (2018). The majority of the 37 genes were encoded by the heavy-strand, except the ND6 gene and eight tRNAs (tRNA-Gln, Ala, Asn, Cys, Tyr, Ser2, Glu, Pro). The intergenic spacers were 33 bp, ranging from 1 to 9 bp in

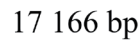


Figure 1 Mitochondrial map of *Psammophis lineolatus*. Genes encoded on the heavy or light strand are indicated on the outside or inside of the circular mitogenome map, respectively, showing the direction of transcription. The tRNAs are denoted by color and labeled according to the three-letter amino acid codes.

size; the longest (9 bp) was located between ND6 and tRNA-Glu. Overlapping nucleotides were found between six pairs of genes, with the length varying from 1 to 25 bp; the largest was located between tRNA-Val and 16S rRNA.

The whole mitogenome of *P. lineolatus* is 17 166 bp in length (Table 1), with A 32%, G 15.5%, T 23.5%, C 29% (Table 2). The strand bias of nucleotide composition of metazoan mitogenomes are usually measured by AT-skews and GC-skews (Perna and Kocher, 1995). The AT-skew and GC-skew of the mitogenome are 0.154 and -0.305, respectively (Table 2), indicating As and Cs are more abundant than Ts and Gs. The nucleotide composition of *P. lineolatus* is obviously inclined to A/T.

3.2. Protein-coding genes and codon usage The total length of the PCGs in mitogenome of *P. lineolatus* was 11 255 bp, which consisted of seven NADH dehydrogenases (ND1–ND6 and ND4L), three cytochrome c oxidases (COX1–COX3), two ATPases (ATP6 and ATP8) and one cytochrome *b* (Cyt b) (Table 1). Herein, five-type starting codons for PCGs were adopted: most start with ATG (COX2, ATP8, ATP6, COX3, ND4L, ND4, ND5, ND6, Cytb), while ND1 with ATA, ND2 with ATT, COX1 with GTG and ND3 with ATC. The majority of the PCGs terminated with TAA, while COX1 used AGG. Five (ND2, COX2, COX3, ND3 and Cytb) terminated with incomplete T, presumably transformed into complete stop codons through post-transcriptional polyadenylation (Ojala *et al.*, 1981).

Table 1 Complete mitochondrial genome of *Psammophis lineolatus* and traits of codon as well as anticodon.

Gene/element	Position		Intergenic nucleotide	Length (bp)	Codon		Anticodon	Stand
	From	To			Start	Stop		
tRNA-Phe	1	66	0	66			GAA	H
12S rRNA	67	991	0	925				H
tRNA-Val	989	1053	-3	65			TAC	H
16S rRNA	1029	2537	-25	1509				H
ND1	2546	3494	8	949	ATA	T--		H
tRNA-Ile	3495	3559	0	65			GAT	H
CR II	3560	4571	0	1012				H
tRNA-Leu ^{UUR} (Leu2)	4572	4644	0	73			TAA	H
tRNA-Gln	4645	4715	0	71			TTG	L
tRNA-Met	4717	4779	1	63			CAT	H
ND2	4780	5806	0	1027	ATT	T--		H
tRNA-Trp	5807	5870	0	64			TCA	H
tRNA-Ala	5873	5938	2	66			TGC	L
tRNA-Asn	5939	6009	0	71			GTT	L
O _L	6012	6049	2	38				
tRNA-Cys	6047	6107	3	61			GCA	L
tRNA-Tyr	6109	6169	1	61			GTA	L
COX1	6171	7772	1	1602	GTG	AGG		H
tRNA-Ser ^{UCN} (Ser2)	7763	7829	0	67			TGA	L
tRNA-Asp	7830	7895	0	66			GTC	H
COX2	7898	8582	2	685	ATG	T--		H
tRNA-Lys	8583	8649	0	66			TTT	H
ATP8	8653	8814	3	162	ATG	TAA		H
ATP6	8805	9484	-10	680	ATG	TA-		H
COX3	9485	10 268	0	784	ATG	T--		H
tRNA-Gly	10 269	10 330	0	62			TCC	H
ND3	10 331	10 676	0	346	ATC	T--		H
tRNA-Arg	10 677	10 741	0	65			TCG	H
ND4L	10 742	11 032	0	291	ATG	TAA		H
ND4	11 033	12 370	0	1338	ATG	TAA		H
tRNA-His	12 371	12 434	0	64			GTG	H
tRNA-Ser ^{AGY} (Ser1)	12 435	12 491	0	57			GCT	H
tRNA-Leu ^{CUN} (Leu1)	12 489	12 559	-3	71			TAG	H
ND5	12 561	14 324	1	1764	ATG	TAA		H
ND6	14 320	14 829	-5	510	ATG	AGG		L
tRNA-Glu	14 839	14 901	9	63			TTC	L
Cytb	14 902	16 018	0	1117	ATG	T--		H
tRNA-Thr	16 016	16 081	-3	66			TGT	H
tRNA-Pro	16 082	16 144	0	63			TGG	L
CR I	16 145	17 166	0	1022				H

Thirteen PCGs contained 3 589 codons without termination codons. The most frequently used amino acids are Leu1 (7.4%), Ser2 (6.3%), and Gly (4.1%), whereas the least common amino acids are Glu (1.8%), Cys (1.7%), Trp (0.18%) (Table 3). The RSCU refers to the relative frequency of each codon to code a specific amino acid, which could measure the bias of codon usage. The RSCU for the mitochondrial PCGs in *P. lineolatus* exhibited an over-usage of A and T at the third codon positions. Among them, AAA-Lys (1.46), CCU-Pro (1.43), ACU-Thr (1.39) and UCA-Ser2 (1.39) are the most frequently used codons. The least

frequent codons are ACG-Thr (0.36), CCG-Pro (0.39) and GCG-Ala (0.49) (Table 3). The AT content of the 12 PCGs (excluding ND6 in the light-strand) is 54.9%; the AT-skew and GC-skew are 0.15 and -0.336, respectively (Table 2), which is also a similar trend in other snakes (Debuy *et al.*, 2012; Wang *et al.*, 2012).

3.3. Transfer and ribosomal RNAs Twenty-two tRNAs were obtained from the complete mitochondrial of *P. lineolatus*. The tRNAs ranged from 57 to 73 bp, and the total length was 1436 bp. There was a positive AT-skew, except in the light-strand tRNA (Table 1; Table 2). The skew analysis of tRNA indicated

Table 2 Composition and skewness of *P. lineolatus* mitogenome.

Regions	Strand	T(U)	C	A	G	AT (%)	GC (%)	AT-skew	GC-skew
Whole genome	H	23.5	29	32	15.5	55.5	44.5	0.154	-0.305
PCGs	H	23.3	30.1	31.6	15	54.9	45.1	0.15	-0.336
tRNAs	H	23.6	25.2	31.9	19.3	55.5	44.5	0.15	-0.133
tRNAs	L	30.2	16.6	24.3	28.9	54.5	45.5	-0.109	0.269
ATP6	H	22.1	30.9	31.8	15.3	53.9	46.2	0.18	-0.338
ATP8	H	16.7	31.5	42.6	9.3	59.3	40.8	0.438	-0.545
COX1	H	25.5	28.1	27.7	18.8	53.2	46.9	0.041	-0.198
COX2	H	22.5	30.1	27	20.4	49.5	50.5	0.091	-0.191
COX3	H	23	30.4	29	17.7	52	48.1	0.115	-0.263
Cytb	H	25.5	30.3	30.3	13.9	55.8	44.2	0.085	-0.372
ND1	H	23.8	30.1	32.5	13.6	56.3	43.7	0.154	-0.378
ND2	H	20.5	31.6	36.2	11.7	56.7	43.3	0.277	-0.461
ND3	H	24.3	30.9	30.6	14.2	54.9	45.1	0.116	-0.372
ND4	H	23.7	30.6	31.8	13.9	55.5	44.5	0.147	-0.375
ND4L	H	26.1	29.2	31.6	13.1	57.7	42.3	0.095	-0.382
ND5	H	22.2	30	34.5	13.2	56.7	43.2	0.217	-0.389
ND6	L	47.3	8	12.2	32.5	59.5	40.5	-0.591	0.604
16S rRNA	H	19.9	24.3	37.7	18.1	57.6	42.4	0.308	-0.146
12S rRNA	H	17.7	26.1	37.2	19	54.9	45.1	0.354	-0.156
CR I	H	31.9	29.2	25	14	56.9	43.2	-0.121	-0.352
CR II	H	31.7	29.1	24.8	14.4	56.5	43.5	-0.122	-0.338

the use of As and Cs in the heavy-strand, while there was an obvious bias toward the use of Ts and Gs in the light-strand (Table 2). All of the tRNAs were able to fold into a typical cloverleaf structure, with the exception of tRNA-Ser^{AGY} and tRNA-Pro, which lacked a dihydrouridine (DHU) arm/stem and TΨC loop, respectively (Figure 2). Lacking the DHU arm/stem is likely related to a compensation mechanism for tRNA transport function – a phenomenon that has been proposed in lizards (Macey *et al.*, 1997; Yu *et al.*, 2018) and toads (Cai *et al.*, 2020). The T arm contraction of snake mitochondrial tRNA has been reported (Kumazawa *et al.*, 1996), and is also notable in *P. lineolatus* mitochondrial tRNA genes, most of which are less than 5 bp (tRNA-Ala, Asp, Glu, His, Lys, Thr) or have only 2-3 bp (tRNA-Gly, Met, Phe). These results suggest that the simplification of mitochondrial tRNA is subject to evolutionary pressure (Kumazawa *et al.*, 1996).

Since there is no reported complete mitogenome in Psammophiidae, we identified the boundaries of rRNA genes based on their relative location in the mitogenome. The 12S rRNA and 16S rRNA genes are 925 bp and 1509 bp in length, respectively, and generally separated by tRNA-Val (Table 1). The AT content of 12S rRNA is 54.9%, and 57.6% in 16S rRNA of *P. lineolatus* (Table 2). The AT-skew of 12S rRNA and 16S rRNA are positive and greater than the GC-skew, suggesting that there are more As and Cs than Ts and Gs (Table 2).

3.4. Control region Duplicate CRs were found in *P. lineolatus* mitogenome. The first CR (CR I; 1022 bp) was located between tRNA-Pro and tRNA-Phe. To date, this is the most typical

position reported for the CR of vertebrate mtDNA. The second CR (CR II; 1012 bp) was located between tRNA-Ile and tRNA-Leu^{UUR} (Leu2) (Figure 1; Table 1). Both CRs were highly conserved in sequence similarity, which could be explained by concerted evolutionary mechanism (Kumazawa *et al.*, 1998). All of their skew values were negative, indicating more Ts and Cs than As and Gs (Table 2).

Three conservative functional domains were observed in both CRs: C-rich, termination-associated sequences (TASs) and conserved sequence blocks (CSBs). The C-rich sequence may facilitate formation of the D-loop by decelerating the extension of heavy-strand synthesis (Kumazawa *et al.*, 1998). The CSBs play an important role in the CR of all organisms, which are associated with the start sites for DNA synthesis. It has been thought that TAS elements are associated with stop sites for DNA synthesis, and have been found near the 3' terminus of the D-loop (Doda *et al.*, 1981). Generally, each control region could find a CSB that presents a CSB-1–CSB-2–CSB-3 arrangement. On the other hand, one or more TASs can appear, and can include forward or reverse complementary sequences. In this study, four types of CR domains arrangements were observed in the Elapodea species (Figure 3; Table S4), and each conserved domain appears only once, rather than, repeatedly. Type A occurred in *P. lineolatus*; Types B and C were assigned to *Naja* spp. and *O. hannah*, respectively; and Type D was assigned to *Bungarus* spp. and *Micrurus fulvius*. These four arrangement types were mostly caused by the change in position of TAS2 and the presence or absence of CSB-2. However, CSB-2

Table 3 Genetic code, amino acid composition and relative synonymous codon usage (RSCU) for the mitochondrial protein-coding genes of *P. lineolatus*.

Codon	Amino acids	Number	Ratio of Codon	RSCU	Codon	Amino acids	Number	Ratio of Codon	RSCU
UUU	Phe	28	0.008	0.78	UAU	Tyr	69	0.019	0.91
UUC		44	0.012	1.22	UAC		83	0.023	1.09
UUA	Leu2	40	0.011	0.71	CAU	His	137	0.038	1.01
UUG		35	0.01	0.62	CAC		135	0.038	0.99
CUU	Leu1	59	0.016	1.04	CAA	Gln	121	0.034	1.38
CUC		63	0.018	1.11	CAG		54	0.015	0.62
CUA		73	0.02	1.29	AAU	Asn	149	0.042	0.97
CUG		70	0.02	1.24	AAC		158	0.044	1.03
AUU	Ile	67	0.019	0.77	AAA	Lys	122	0.034	1.46
AUC		107	0.03	1.23	AAG		45	0.013	0.54
AUA	Met	70	0.02	1.36	GAU	Asp	32	0.009	0.85
AUG		33	0.009	0.64	GAC		43	0.012	1.15
GUU	Val	20	0.006	0.87	GAA	Glu	38	0.011	1.21
GUC		23	0.006	1	GAG		25	0.007	0.79
GUA		20	0.006	0.87	UGU	Cys	31	0.009	1.05
GUG		29	0.008	1.26	UGC		28	0.008	0.95
UCU	Ser2	70	0.02	1.28	UGA	Trp	26	0.007	0.8
UCC		51	0.014	0.93	UGG		39	0.011	1.2
UCA		76	0.021	1.39	CGU	Arg	22	0.006	0.75
UCG		28	0.008	0.51	CGC		41	0.011	1.39
CCU	Pro	120	0.033	1.43	CGA		26	0.007	0.88
CCC		95	0.026	1.13	CGG		29	0.008	0.98
CCA		87	0.024	1.04	AGU	Ser1	30	0.008	0.55
CCG		33	0.009	0.39	AGC		74	0.021	1.35
ACU	Thr	141	0.039	1.39	GGU	Gly	27	0.008	0.74
ACC		92	0.026	0.9	GGC		46	0.013	1.27
ACA		137	0.038	1.35	GGA		23	0.006	0.63
ACG		37	0.01	0.36	GGG		49	0.014	1.35
GCU	Ala	41	0.011	1.18	UAA	*	0	0	0
GCC		47	0.013	1.35	UAG	*	0	0	0
GCA		34	0.009	0.98	AGA	*	0	0	0
GCG		17	0.005	0.49	AGG	*	0	0	0

* Stop (termination) codon excluded.

Note: Ratio of codon is equal to the number of each codon divided by the total number of codons (3589).

cannot be found in *P. lineolatus*, *M. fulvius* and *Bungarus* spp. A similar finding was reported in previous studies (Dong and Kumazawa, 2005; Kumazawa, 2004). At present, the mechanism determining the presence or absence of CSB-2, and whether it has phylogenetic significance, is still unclear. The motif sequence of CSB-1 was highly similar in snake species, while the CSB-3 motif was rarely conserved in previous studies (Kumazawa *et al.*, 1996; Kumazawa *et al.*, 1998; Dong and Kumazawa, 2005; Douglas *et al.*, 2006). Hence, the recognition of CSB-3 was very difficult or ambiguous. Comparison of the CSB-3 motif of *Naja atra* (Qian, 2018) and the two CRs of *P. lineolatus* and the other Elapidae snakes (Figure 3; Table S4) revealed that the CSB-3 motif is identical in *P. lineolatus* and *Naja* spp., but slightly different in other Elapidae. Notably, the CSB-3 motif of *N. atra* was located between TASI and CSB-1 to form a CSB-3–CSB-1–CSB-2 order (Qian, 2018) rather than the

common CSB-1–CSB-2–CSB-3 structure. This arrangement was different than that reported in previous studies of snakes (Kumazawa *et al.*, 1998; Dong and Kumazawa, 2005; Douglas *et al.*, 2006) and other vertebrates (Sbisa *et al.*, 1997). The TAS motifs of the eight species (incorporating TASI and TAS2) were almost identical to those reported in other snakes (Kumazawa *et al.*, 1998). No tandem repeats were discovered, while a poly T sequence (5'-TTTTTTTT-3') was detected at both CRs within Elapoidea. These length variations are only seen in regions of simple repeats of a nucleotide or dinucleotide, suggesting that replicational slippage (Levinson and Gutman, 1987) plays a role in creating length mutations.

3.5. Ka/Ks ratio The Ka/Ks ratios of the 13 PCGs varied from 0.027 to 0.680, but were always less than 1, indicating that these genes are evolving under purifying selection (Figure 4). Within all compared mitogenomes, the highest average of Ka/Ks ratio

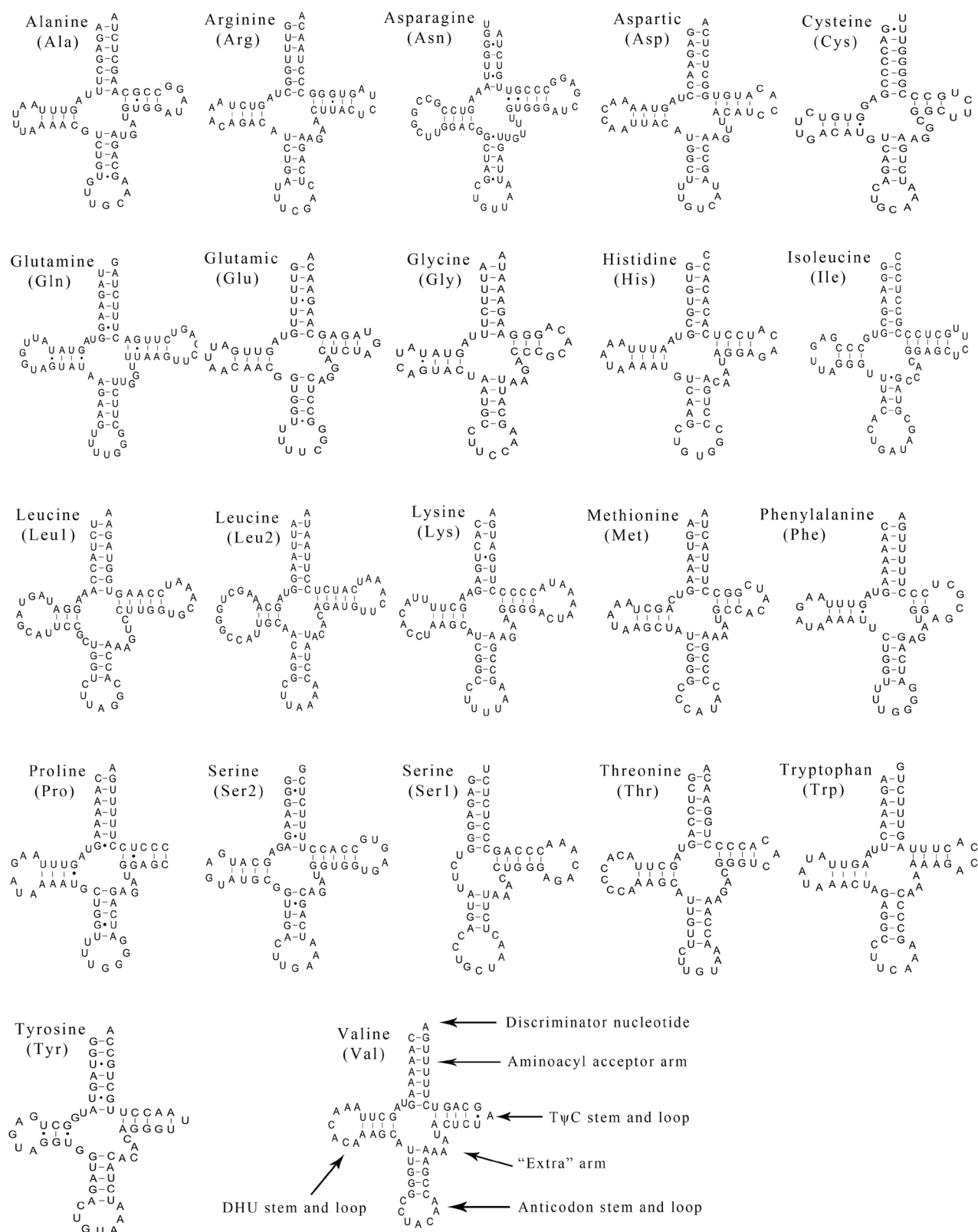


Figure 2 Putative secondary structures of the 22 tRNAs identified in the mitogenome of *Psammophis lineolatus*. The tRNAs are labeled with their corresponding three-letter amino acid codes. Dashed line (–) indicates Watson-Crick base pairing and solid dots (•) between G and U pairs mark canonical base pairings appearing in RNA.

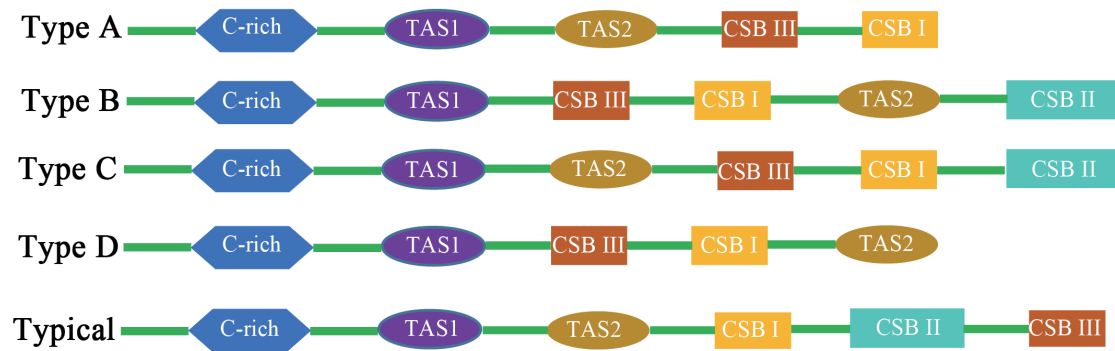


Figure 3 Arrangement of the mitochondrial control region structure of eight snake species of the Elapoidea superfamily, with the typical arrangement of vertebrates for comparison. Green represents other regions of the control region. Type A: *Psammophis lineolatus*. Type B: *Naja naja*, *Naja kaouthia*, *Naja atra*. Type C: *Ophiophagus Hannah*. Type D: *Micrurus fulvius*, *Bungarus fasciatus* and *Bungarus multicinctus*.

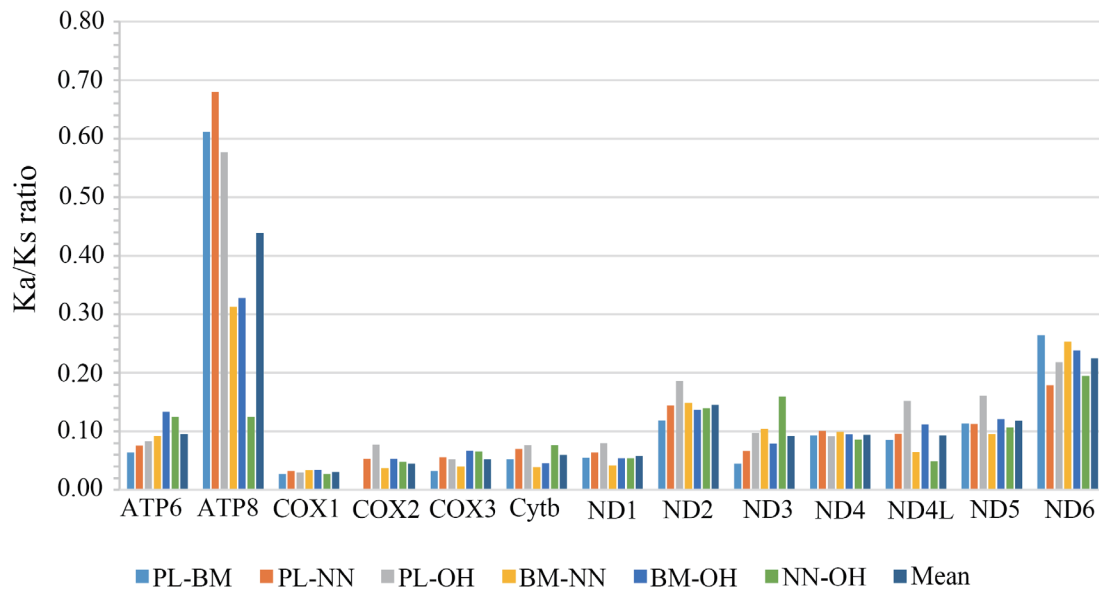


Figure 4 Non-synonymous (Ka) and synonymous (Ks) substitution ratio of comparisons between *Psammophis lineolatus* and the other three Elapidae species. BM: *Bungarus multicinctus*; NN: *Naja naja*; OH: *Ophiophagus hannah*; PL: *P. lineolatus*.

was observed for ATP8, while COX1 had the lowest ratio. ATP8 was indicated to be under positive or relaxed selection pressure, which has also been reported in other vertebrates (Sun *et al.*, 2020). On the other hand, the low Ka/Ks ratio of COX1 is indicative of strong purifying selection, which is in accordance with results reported in *Python* snakes (Dubey *et al.*, 2012). Importantly, the Ks value of COX2 for *P. lineolatus*-*B. multicinctus* (PL-BM) was not applicable. This arose because the Jukes and Cantor correction cannot be calculated when the proportion of differences is equal or higher than 0.75 (Rozas *et al.*, 2017).

3.6. Phylogenetic analyses Both BI and ML approaches provided identical and well-supported tree topologies. Thus, only the BI tree is presented, which includes PP as well as UFBoot from ML (Figure 5). With limited taxon sampling, monophyly of the Caenophidia (advanced snakes) was recovered with strong support (PP = 1.0; UFBoot = 100), which is largely consistent with results of recent studies (Greiner *et al.*, 2019; Pyron *et al.*, 2011; Pyron *et al.*, 2014; Reeder *et al.*, 2015; Wiens *et al.*, 2012; Zheng and Wiens, 2016). In the Caenophidia, Acrochordidae was recovered as the sister taxon, followed successively by Xenodermatidae, Viperidae, Homalopsidae,

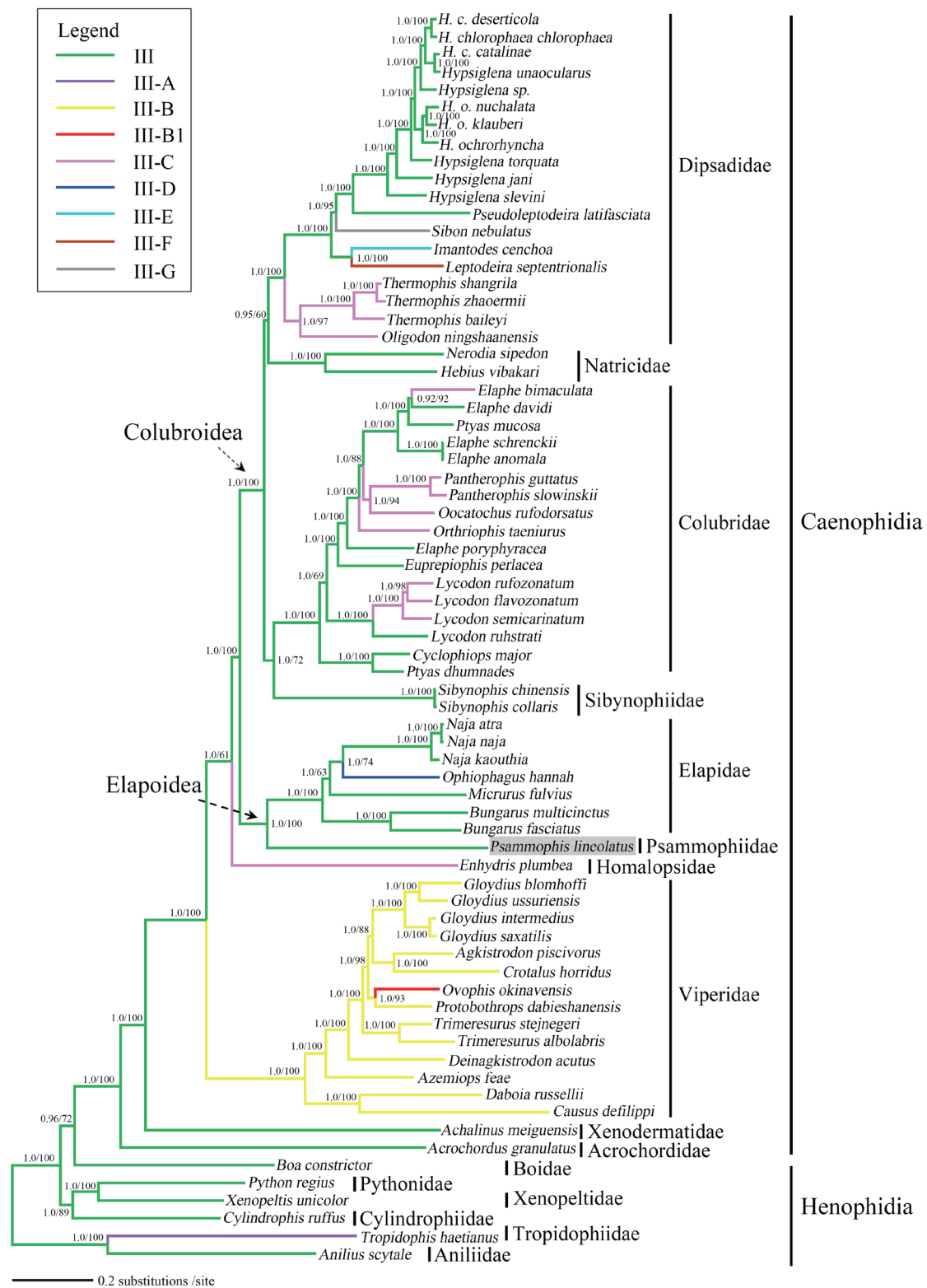


Figure 5 A majority-rule consensus tree inferred from Bayesian inference using MrBayes v3.2, based on the combined data set of RNA genes and protein-coding genes. The phylogenetic position of Psammophiidae is highlighted in gray. Numbers beside the nodes indicate Bayesian posterior probabilities (PP) and ML ultrafast bootstrap values (UFBoot), respectively. Branch lengths represent means of posterior distribution. Family/superfamily/group assignments are listed. Types III to III-G correspond to the nine types of mitochondrial gene arrangement patterns as designated in Qian *et al.* (2018).

Elapoidea and Colubroidae. These results also align with recent studies (Streicher and Wiens, 2016; Zaher *et al.*, 2019). Monophyly of both the Elapoidea and Colubroidae superfamilies was recovered with strong support (PP = 1.0; UFBoot = 100). Notably, in the sampled lineages, Psammophiidae was clustered into the Elapoidea superfamily (PP = 1.0; UFBoot = 100). Nevertheless, according to recent phylogenetic studies (Figueroa *et al.*, 2016; Kelly *et al.*, 2009; Zaher *et al.*, 2019), which were based on analyses of a few mitochondrial and/or nuclear genes, the sister taxon of Psammophiidae is unclear. Thus, it is necessary to add more taxa and mitogenome sequences to explore the phylogenetic relationships of the advanced snakes in general, and to resolve the phylogenetic position of Psammophiidae in Elapoidea in particular.

Acknowledgments We thank Prof. Dali Chen (Sichuan University) and Mr. Song Wang for assistance with fieldwork in Xinjiang Uygur Autonomous Region, China. We also thank two anonymous referees for comments that improved the clarity of an earlier version of this manuscript. We are grateful to Dr. Jacquelin De Faveri for English editing. This study was supported by the National Natural Science Foundation of China (Nos. 31672270, 32070433). Jun Li was supported by grant from the National Natural Science Foundation of China (No. 31560591).

References

- Bernt M., Bleidorn C., Braband A., Dambach J., Donath A., Fritzsche G., Golombek A., Hadrys H., Jühling F., Meusemann K., Middendorf M., Misof B., Perseke M., Podsiadlowski L., von Reumont B., Schierwater B., Schlegel M., Schrödl M., Simon S., Stadler P. F., Stöger I., Struck T. H. 2013a. A comprehensive analysis of bilaterian mitochondrial genomes and phylogeny. *Mol Phylogenet Evol*, 69: 352–364
- Bernt M., Braband A., Schierwater B., Stadler P. F. 2013b. Genetic aspects of mitochondrial genome evolution. *Mol Phylogenet Evol*, 69: 328–338
- Bernt M., Donath A., Jühling F., Externbrink F., Florentz C., Fritzsche G., Pütz J., Middendorf M., Stadler P. F. 2013c. MITOS: Improved *de novo* metazoan mitochondrial genome annotation. *Mol Phylogenet Evol*, 69: 313–319
- Boore J. L. 1999. Animal mitochondrial genomes. *Nucleic Acids Res*, 27: 1767–1780
- Boore J. L., Brown W. M. 1998. Big trees from little genomes: mitochondrial gene order as a phylogenetic tool. *Curr Opin Genet Dev*, 8: 668–674
- Bourgeois M. 1968. Contribution à la morphologie comparée du crâne des Ophidiens de l'Afrique Centrale. Publications de l'Université Officielle du Congo vol. XVIII: 1–293
- Brandt J. F. 1838. Note sur quatre nouvelles espèces de serpents de la côte occidentale de la mer Caspienne et de la Perse septentrionale, découvertes par M. Kareline; par M. Brandt (in le 22 décembre 1837). *Bulletin de l'Académie Impériale des Sciences de Saint Pétersbourg*, 3: 241–244
- Cai Y., Li Q., Zhang J., Storey K. B., Yu D. 2020. Characterization of the mitochondrial genomes of two toads, *Anaxyrus americanus* (Anura: Bufonidae) and *Bufotes pewzowi* (Anura: Bufonidae), with phylogenetic and selection pressure analyses. *PeerJ*, 8: e8901
- Chen N., Zhao S. 2009. New progress in snake mitochondrial gene rearrangement. *Mitochondrial DNA*, 20: 69–71
- Doda J. N., Wright C. T., Clayton D. A. 1981. Elongation of displacement-loop strands in human and mouse mitochondrial DNA is arrested near specific template sequences. *Proc Natl Acad Sci USA*, 78: 6116–6120
- Dong S., Kumazawa Y. 2005. Complete mitochondrial DNA sequences of six snakes: phylogenetic relationships and molecular evolution of genomic features. *J Mol Evol*, 61: 12–22
- Douglas D. A., Gower D. J. 2010. Snake mitochondrial genomes: phylogenetic relationships and implications of extended taxon sampling for interpretations of mitogenomic evolution. *BMC Genomics*, 11: 14
- Douglas D. A., Jank A., Arnason U. 2006. A mitogenomic study on the phylogenetic position of snakes. *Zool Scr*, 35: 545–558
- Dowling H. G., Duellman W. E. 1978. Systematic herpetology: A synopsis of families and higher categories. HISS Publications, New York
- Dubey B., Meganathan P. R., Haque I. 2012. Complete mitochondrial genome sequence from an endangered Indian snake, *Python molurus molurus* (Serpentes, Pythonidae). *Mol Biol Rep*, 39: 7403–7412
- Figueroa A., McKelvey A. D., Grismer L. L., Bell C. D., Lailvaux S. P. 2016. A species-level phylogeny of extant snakes with description of a new colubrid subfamily and genus. *PLoS ONE*, 11: e0161070
- Gouy M., Guindon S., Gascuel O. 2010. SeaView version 4: a multiplatform graphical user interface for sequence alignment and phylogenetic tree building. *Mol Biol Evol*, 27: 221–224
- Gravlund P. 2001. Radiation within the advanced snakes (Caenophidia) with special emphasis on African *Opisthophis colubrids*, based on mitochondrial sequence data. *Biol J Linn Soc*, 72: 99–114
- Greiner S., Lehmark P., Bock R. 2019. OrganellarGenomeDRAW (OGDRAW) version 1.3.1: expanded toolkit for the graphical visualization of organellar genomes. *Nucleic Acids Res*, 47: W59–W64
- Hurst L. D. 2002. The Ka/Ks ratio: diagnosing the form of sequence evolution. *Trends Genet*, 18: 486–487
- Hurst L. D. 2009. Evolutionary genomics and the reach of selection. *J Biol*, 8: 12
- Jiang Z. J., Castoe T. A., Austin C. C., Burbrink F. T., Herron M. D., McGuire J. A., Parkinson C. L., Pollock D. D. 2007. Comparative mitochondrial genomics of snakes: extraordinary substitution rate dynamics and functionality of the duplicate control region. *BMC Evol Biol*, 7: 123
- Katoh K., Standley D. M. 2013. MAFFT multiple sequence alignment software version 7: improvements in performance and usability. *Mol Biol Evol*, 30: 772–780
- Kelly C. M. R., Barker N. P., Villet M. H. 2003. Phylogenetics of advanced snakes (Caenophidia) based on four mitochondrial genes. *Syst Biol*, 52: 439–459
- Kelly C. M. R., Barker N. P., Villet M. H., Broadley D. G., Branch W. R. 2008. The snake family Psammophiidae (Reptilia: Serpentes): Phylogenetics and species delimitation in the African sand snakes (*Psammophis* Boie, 1825) and allied genera. *Mol Phylogenet Evol*, 47: 1045–1060
- Kelly C. M. R., Barkera N. P., Villet M. H., Broadley D. G. 2009. Phylogeny, biogeography and classification of the snake superfamily Elapoidea: a rapid radiation in the late Eocene. *Cladistics*, 25: 38–63
- Knaus B. J., Cronn R., Liston A., Pilgrim K., Schwartz M. K. 2011. Mitochondrial genome sequences illuminate maternal lineages of conservation concern in a rare carnivore. *BMC Ecol*, 11: 10
- Kumar S., Stecher G., Tamura K. 2016. MEGA7: molecular evolutionary genetics analysis version 7.0 for bigger datasets. *Mol Biol Evol*, 33:

1870–1874

- Kumazawa Y. 2004. Mitochondrial DNA sequences of five squamates, phylogenetic affiliation of snakes. *DNA Res*, 11: 137–144
- Kumazawa Y., Ota H., Nishida M., Ozawa T. 1996. Gene rearrangements in snake mitochondrial genomes, highly concerted evolution of control region-like sequences duplicated and inserted into a tRNA gene cluster. *Mol Biol Evol*, 13: 1242–1254
- Kumazawa Y., Ota H., Nishida M., Ozawa T. 1998. The complete nucleotide sequence of a snake (*Dinodon semicarinatus*) mitochondrial genome with two identical control regions. *Genetics*, 150: 313–329
- Lanfear R., Frandsen P. B., Wright A. M., Senfeld T., Calcott B. 2017. PartitionFinder 2: New methods for selecting partitioned models of evolution for molecular and morphological phylogenetic analyses. *Mol Biol Evol*, 34: 772–773
- Lawson R., Slowinski J. B., Crother B. L., Burbrink F. T. 2005. Phylogeny of the Colubroidea (Serpentes): New evidence from mitochondrial and nuclear genes. *Mol Phylogenet Evol*, 37: 581–601
- Levinson G., Gutman G. A. 1987. Slipped-strand mispairing: A major mechanism for DNA sequence evolution. *Mol Biol Evol*, 4: 203–221
- Lowe T. M., Chan P. P. 2016. tRNAscan-SE On-line: integrating search and context for analysis of transfer RNA gene. *Nucleic Acids Res*, 44: W54–W57
- Macey J. R., Larson A., Ananjeva N. B., Fang Z., Papenfuss T. J. 1997. Two novel gene orders and the role of light-strand replication in rearrangement of the vertebrate mitochondrial genome. *Mol Biol Evol*, 14: 91–104
- Mauro D. S., Gower D. J., Zardoya R., Wilkinson M. 2006. A hotspot of gene order rearrangement by tandem duplication and random loss in the vertebrate mitochondrial genome. *Mol Biol Evol*, 23: 227–234
- Minh B. Q., Nguyen M. A. T., Haeseler A. V. 2013. Ultrafast approximation for phylogenetic bootstrap. *Mol Biol Evol*, 30: 1188–1195
- Nagy Z. T., Joger U., Wink M., Glaw F., Vences M. 2003. Multiple colonization of Madagascar and Socotra by colubrid snakes: evidence from nuclear and mitochondrial gene phylogenies. *Proc Biol Sci*, 270: 2613–2621
- Nguyen L., Schmidt H. A., Arndt V. H., Minh B. Q. 2015. IQ-TREE: a fast and effective stochastic algorithm for estimating maximum likelihood phylogenies. *Mol Biol Evol*, 32: 268–274
- Ojala D., Montoya J., Attardi G. 1981. tRNA punctuation model of RNA processing in human mitochondria. *Nature*, 290: 470–474
- Okajima Y., Kumazawa Y. 2010. Mitochondrial genomes of acrodont lizards: timing of gene rearrangements and phylogenetic and biogeographic implications. *BMC Evol Biol*, 10: 141
- Pereira S. L. 2000. Mitochondrial genome organization and vertebrate phylogenetics. *Genet Mol Biol*, 23: 745–752
- Perna N. T., Kocher T. D. 1995. Patterns of nucleotide composition at fourfold degenerate sites of animal mitochondrial genomes. *J Mol Evol*, 41: 353–358
- Pruitt K. D., Tatusova T., Maglott D. R. 2007. NCBI reference sequences (RefSeq): A curated non-redundant sequence database of genomes, transcripts and proteins. *Nucleic Acids Res*, 35: D61–D65
- Pyron R. A., Burbrink F. T., Colli G. R., de Oca A. N. M., Vitt L. J., Kuczynski C. A., Wiens J. J. 2011. The phylogeny of advanced snakes (Colubroidea), with discovery of a new subfamily and comparison of support methods for likelihood trees. *Mol Phylogenet Evol*, 58: 329–342
- Pyron R. A., Hendry C. R., Chou V. M., Lemmon E. M., Lemmon A. R., Burbrink F. T. 2014. Effectiveness of phylogenomic data and coalescent species-tree methods for resolving difficult nodes in the phylogeny of advanced snakes (Serpentes: Caenophidia). *Mol Phylogenet Evol*, 81: 221–231
- Qian L. 2018. Evolution of the mitochondrial genome structure in snake, with the biogeography analysis of *Protophthops*. Doctoral Dissertation, Anhui University, Hefei, Anhui Province, China (In Chinese with English abstract)
- Qian L., Wang H., Yan J., Pan T., Jiang S., Rao D., Zhang B. 2018. Multiple independent structural dynamic events in the evolution of snake mitochondrial genomes. *BMC Genomics*, 19: 354
- Raina S. Z., Faith J. J., Disotell T. R., Seligmann H., Stewart C., Pollock D. D. 2005. Evolution of base-substitution gradients in primate mitochondrial genomes. *Genome Res*, 15: 665–673
- Reeder T. W., Townsend T. M., Mulcahy D. G., Noonan B. P., Wood Jr P. L., Sites Jr J. W., Wiens J. J. 2015. Integrated analyses resolve conflicts over squamate reptile phylogeny and reveal unexpected placements for fossil taxa. *PLoS ONE*, 10: e0118199
- Ronquist F., Teslenko M., Mark P. V. D., Ayres D. L., Darling A., Höhna S., Larget B., Liu L., Suchard M. A., Huelsenbeck J. P. 2012. MrBayes 3.2: efficient Bayesian phylogenetic inference and model choice across a large model space. *Syst Biol*, 61: 539–542
- Rozas J., Ferrer-Mata A., Sánchez-DelBarrio J. C., Guirao-Rico S., Librado P., Ramos-Onsins S. E., Sánchez-Gracia A. 2017. DnaSP 6: DNA sequence polymorphism analysis of large data sets. *Mol Biol Evol*, 34: 3299–3302
- Sbisa E., Tanzariello F., Reyes A., Pesole G., Saccone C. 1997. Mammalian mitochondrial D-loop region structural analysis: Identification of new conserved sequences and their functional and evolutionary implications. *Gene*, 205: 125–140
- Streicher J. W., Wiens J. J. 2016. Phylogenomic analyses reveal novel relationships among snake families. *Mol Phylogenet Evol*, 100: 160–169
- Sun C., Liu H., Lu C. 2020. Five new mitogenomes of *Phylloscopus* (Passeriformes, Phylloscopidae): Sequence, structure, and phylogenetic analyses. *Int J Biol Macromol*, 146: 638–647
- Uetz P., Freed P., Hošek J. 2020. The Reptile Database, <http://www.reptile-database.org> (accessed 1st October 2020)
- Vidal N., Hedges S. B. 2002a. Higher-level relationships of snakes inferred from four nuclear and mitochondrial genes. *C R Biol*, 325: 977–985
- Vidal N., Hedges S. B. 2002b. Higher-level relationships of caenophidian snakes inferred from four nuclear and mitochondrial genes. *C R Biol*, 325: 987–995
- Wang G. L., He S. P., Huang S., He M., Zhao E. M. 2009. The complete mitochondrial DNA sequence and the phylogenetic position of *Achalina meiguensis* (Reptilia: Squamata). *Chin Sci Bull*, 54: 1713–1724
- Wiens J. J., Hutter C. R., Mulcahy D. G., Noonan B. P., Townsend T. M., Sites Jr J. W., Reeder T. W. 2012. Resolving the phylogeny of lizards and snakes (Squamata) with extensive sampling of genes and species. *Biol Lett*, 8: 1043–1046
- Wilcox T. P., Zwickl D. J., Heath T. A., Hillis D. M. 2002. Phylogenetic relationships of the dwarf boas and a comparison of Bayesian and bootstrap measures of phylogenetic support. *Mol Phylogenet Evol*, 25: 361–371
- Xia Y., Zheng Y., Miura I., Wong P. B. Y., Murphy R. W., Zeng X. 2014. The evolution of mitochondrial genomes in modern frogs (Neobatrachia): nonadaptive evolution of mitochondrial genome reorganization. *BMC Genomics*, 15: 691
- Xia Y., Zheng Y., Murphy R. W., Zeng X. 2016. Intraspecific rearrangement of mitochondrial genome suggests the prevalence of the tandem duplication random loss (TDLR) mechanism in *Quasipaa boulengeri*.

- BMC Genomics, 17: 965
- Yan J., Li H., Zhou K. 2008. Evolution of the mitochondrial genome in snakes: Gene rearrangements and phylogenetic relationships. BMC Genomics, 9: 569
- Yang Z., Bielawski J. P. 2000. Statistical methods for detecting molecular adaptation. Trends Ecol Evol, 15: 496–503
- Yu X., Du Y., Fang M., Li H., Lin L. 2018. The mitochondrial genome of *Pseudocalotes microlepis* (Squamata: Agamidae) and its phylogenetic position in agamids. Asian Herpetol Res, 9: 24–34
- Zaher H. 1999. Hemipenial morphology of the South American Xenodontine snakes, with a proposal for a monophyletic Xenodontinae and a reappraisal of colubroid hemipenes. Bull Am Mus Nat Hist, 240: 1–168
- Zaher H., Murphy R. W., Arredondo J. C., Graboski R., Machado-Filho P. R., Mahlow K., Montingelli G. G., Quadros A. B., Orlov N. L., Wilkinson M., Zhang Y. P., Grazziotin F. G. 2019. Large-scale molecular phylogeny, morphology, divergence-time estimation, and the fossil record of advanced caenophidian snakes (Squamata: Serpentes). PLoS ONE, 14: e0216148
- Zheng Y., Wiens J. J. 2016. Combining phylogenomic and supermatrix approaches, and a time-calibrated phylogeny for squamate reptiles (lizards and snakes) based on 52 genes and 4162 species. Mol Phylogenet Evol, 94: 537–557

Handling Editor: Heling Zhao

How to cite this article:

Chen M. L., Liu J. L., Li J., Wu N., Guo X. G. Complete Mitochondrial Genome of the Steppe Ribbon Racer (*Psammophis lineolatus*): The First Representative from the Snake Family Psammophiidae and its Phylogenetic Implications. Asian Herpetol Res, 2021, 12(3): 295–307. DOI: 10.16373/j.cnki.ahr.200129

Appendix

Table S1 PCR primers for amplification of the complete mitochondrial genome of *Psammophis lineolatus*.

No.	Primer name	5'—3' sequence	Annealing temperature (°C) used in the PCR	Approximate product length (bp)	References
1	ul2S-1L	GCGCACACACCGCCCGTC	55	1400	Kumazawa and Endo (2004)
	16S-R2	CCATYAGGATGTCCTGATCC			
2	A12F	GCAACGCCTGCCAGTGAACAATT	47.5	900	This study
	ND1-P3r	AATCGHGGGTAKGANGCTCG			
3	ND1-P2	TCATGACCNITAGCCATAAT	50.0	1600	This study
	Met-R2	GGTATGGGCCCGARMTAGCTT			
4	Met-F1	GGCCGTGCAAAAGGCTTAAACC	55.0	700	This study
	ND2-P2r	GAKGAGAAWGCTATTAGYTTTCG			
5	ND2-P1	TGAYTACCAGAAGTVDCACAAGG	50.0	1500	This study
	CO1-P3r	GGATTGADGADGDCDCCTGC			
6	CO1-P1	TCACTATTTGGCAGCGACCAGA	50.0	1600	This study
	CO2-P1r	GTAGGAAGAYRACYTCTTCTAT			
7	CO1-P4	GTCATAGCCAAGTTACATCC	56.0	770	This study
	CO2-P2r	TGSGGCATTTCACTAAGGAA			
8	CO2-P1	ATAGAAGARGTYRTCTTCCTAC	50.0	1700	This study
	CO3-P1r	CATGGGCTBGGGTCWACWAGATG			
9	B169F	CTCACAGCAAATATTACGGCG	50.5	600	This study
	B169R	GATCATGTAATTGTTGCTCCG			
10	CO3-P1	CATCTWGTWGACCCVAGCCCATG	55.0	900	Kumazawa and Endo (2004)
	ND3-P1r	GGRTCRAAGCCGCAYTCRTA			
11	CO3-P2	ATGCCTTCCAAGCATTAAG	55.0	400	This study
	GLr	GTTCTTCTGAGTCGAAATCAG			
12	ND3-P1	TAYGARTGCGGCTTYGAYCC	55.0	1500	Kumazawa and Endo (2004)
	ND4-P2r	TTTGCTAGRCAGAAWAGTGC			
13	ND4-P1	TACTCHTCWRTHAGCCACAT	55.0	1400	Kumazawa and Endo (2004)
	ND5-P1r	ACAACTATKGTRCTRGARTG			
14	ND4-P3	TGTGRCCCTGACAATAGGA	55.0	1300	Kumazawa and Endo (2004)
	ND5-P2r	ATDGTGTCTTTTGARTAGAAAMCC			
15	ND5-P2	GGKTTCTAYTCAAAAGACACHAT	55.0	1300	Kumazawa and Endo (2004)
	Cytb-P1r	AGGCAGGTTAGTAGTATGGA			
16	rcytb-1H	GCGTAGGCRAATAGGAAGTATCA	53.4	800	Kumazawa and Endo (2004)
	rGlu-1L	GAAAAACCRCCGTTGTWATTCAACTA			
17	Cytb-P1	TCCATACTACTAACCTGCCT	55.0	600	Kumazawa and Endo (2004)
	Cytb-P3r	TTDGAGAARTTTTCTGGGTC			
18	Cytb-P1	TCCATACTACTAACCTGCCT	53.9	1100	This study
	E1417R	GTATATGCCAGGCCAAGAA			
19	rThr-2L	YAAAGCMTTGRCTTGTA	56.1	1100	Kumazawa and Endo (2004)
	rCONT-4H	CTCGKTTTWGGGGTTTGRCA			
20	rThr-2L	YAAAGCMTTGRCTTGTA	52.0	1900	Kumazawa and Endo (2004)
	CHr	CTGTTGATCGCATCTACT			

References

Kumazawa Y., Endo H. 2004. Mitochondrial genome of the Komodo dragon: Efficient sequencing method with reptile-oriented primers and novel gene rearrangements. *DNA Res*, 11: 115–125

Table S2 Summary of taxonomic groups used in this study, including GenBank accession numbers

Family	Species	Accession number	References
Ingroup			
Acrochordidae	<i>Acrochordus granulosus</i>	AB177879	Dong and Kumazawa (2015)
Xenodermatidae	<i>Achalinus meiguensis</i>	FJ424614	Dong and Kumazawa (2015)
Viperidae	<i>Causus defilippi</i>	GU045452	Castoe <i>et al.</i> (2009)
	<i>Daboia russellii</i>	EU913478	Chen and Zhao (2009)
	<i>Azemiops feae</i>	KJ872487	Geng and Yan (Unpubl. data)
	<i>Deinagkistrodon acutus</i>	DQ343647	Yan <i>et al.</i> (2008)
	<i>Trimeresurus albolabris</i>	KF311102	Song <i>et al.</i> (2015)
	<i>Trimeresurus stejnegeri</i>	FJ752492	Lin <i>et al.</i> (Unpubl. data)
	<i>Protobothrops dabieshanensis</i>	KF003004	Huang <i>et al.</i> (2014)
	<i>Ovophis okinavensis</i>	AB175670	Dong and Kumazawa (2015)
	<i>Crotalus horridus</i>	HM641837	Hall <i>et al.</i> (2013)
	<i>Agkistrodon piscivorus</i>	DQ523161	Jiang <i>et al.</i> (2007)
	<i>Gloydius saxatilis</i>	KM434236	Xu <i>et al.</i> (2015a)
	<i>Gloydius intermedius</i>	KM186844	Xu <i>et al.</i> (2015b)
	<i>Gloydius brevicaudus</i>	EU913477	Chen and Zhao (2009)
	<i>Gloydius ussuriensis</i>	KP262412	Han <i>et al.</i> (2015)
Homalopsidae	<i>Enhydryis plumbea</i>	DQ343650	Yan <i>et al.</i> (2008)
Psammophiidae	<i>Psammophis lineolatus</i>	MT991050	This study
Elapidae	<i>Bungarus fasciatus</i>	EU579523	Chen and Zhao (2009)
	<i>Bungarus multicinctus</i>	EU579522	Chen and Zhao (2009)
	<i>Micrurus fulvius</i>	GU045453	Castoe <i>et al.</i> (2009)
	<i>Ophiophagus hannah</i>	EU921899	Chen and Zhao (2009)
	<i>Naja kaouthia</i>	LC431744	Singchat <i>et al.</i> (2019)
	<i>Naja naja</i>	DQ343648	Yan <i>et al.</i> (2008)
	<i>Naja atra</i>	EU913475	Chen and Zhao (2009)
Sibynophiidae	<i>Sibynophis collaris</i>	JN211315	Jiang and Hwang (2011)
	<i>Sibynophis chinensis</i>	KF360246	Oh <i>et al.</i> (2014)
Colubridae	<i>Ptyas dhumnades</i>	KF148621	Li <i>et al.</i> (Unpubl. data)
	<i>Cyclophiops major</i>	KF148620	Sun <i>et al.</i> (2017)
	<i>Lycodon ruhstrati</i>	KJ179951	Qian <i>et al.</i> (2018)
	<i>Lycodon semicarinatum</i>	AB008539	Qian <i>et al.</i> (2018)
	<i>Lycodon rufozonatum</i>	KJ179950	Qian <i>et al.</i> (2018)
	<i>Lycodon flavozonatum</i>	KR911720	Qian <i>et al.</i> (2018)
	<i>Euprepophis perlacea</i>	KF750656	Wan <i>et al.</i> (2016)
	<i>Elaphe poryphyracea</i>	GQ181130	Lin <i>et al.</i> (Unpubl. data)
	<i>Orthriophis taeniurus</i>	KC990021	Li <i>et al.</i> (2016)
	<i>Oocatochus rufodorsatus</i>	KC990020	Li <i>et al.</i> (2014)
	<i>Pantherophis slowinskii</i>	DQ523162	Jiang <i>et al.</i> (2007)
	<i>Pantherophis guttatus</i>	AM236349	Douglas <i>et al.</i> (2006)
	<i>Elaphe anomala</i>	KP900218	Liu and Zhao (2016)
	<i>Elaphe schrenckii</i>	KP888955	Liu and Zhao (2015)
	<i>Ptyas mucosa</i>	KT982276	Zhou <i>et al.</i> (2016)
	<i>Elaphe davidi</i>	KM401547	Xu <i>et al.</i> (2016a)
	<i>Elaphe bimaculata</i>	KM065513	Yan <i>et al.</i> (2016)
Natricidae	<i>Hebius vibakari</i>	KP684155	Xu <i>et al.</i> (2016b)
	<i>Nerodia sipedon</i>	JF964960	Huff <i>et al.</i> (Unpubl. data)
Dipsadidae	<i>Oligodon ningshaanensis</i>	KJ719252	Wang (2014)
	<i>Thermophis baileyi</i>	MF326642	Sun (2017)
	<i>Thermophis zhaoermii</i>	GQ166168	He <i>et al.</i> (2010)
	<i>Thermophis shangrila</i>	MF066951	He <i>et al.</i> (2010)
	<i>Leptodeira septentrionalis</i>	EU728590	Mucahy and Macey (2009)
	<i>Imantodes cenchoa</i>	EU728586	Mucahy and Macey (2009)
	<i>Sibon nebulatus</i>	EU728583	Mucahy and Macey (2009)
	<i>Pseudoleptodeira latifasciata</i>	EU728579	Mucahy and Macey (2009)
	<i>Hypsiglena slevini</i>	EU728584	Mucahy and Macey (2009)

Continued Table S2

Family	Species	Accession number	References
	<i>Hypsiglena jani</i>	EU728592	Mucahy and Macey (2009)
	<i>Hypsiglena torquata</i>	EU728591	Mucahy and Macey (2009)
	<i>H. ochrorhyncha ochrorhyncha</i>	EU728578	Mucahy and Macey (2009)
	<i>H. o. klauberi</i>	EU728589	Mucahy and Macey (2009)
	<i>H. o. nuchalata</i>	EU728581	Mucahy and Macey (2009)
	<i>Hypsiglena</i> sp.	EU728580	Mucahy and Macey (2009)
	<i>Hypsiglena unaocularis</i>	KJ486458	Mucahy <i>et al.</i> (2014)
	<i>H. chlorophaea chlorophaea</i>	EU728593	Mucahy and Macey (2009)
	<i>H. c. catalinae</i>	KJ486459	Mucahy <i>et al.</i> (2014)
	<i>H. c. deserticola</i>	EU728587	Mucahy and Macey (2009)
Outgroup			
Aniliidae	<i>Anilius scytale</i>	FJ755180	Castoe <i>et al.</i> (2009)
Tropidophiidae	<i>Tropidophis haetianus</i>	FJ755181	Castoe <i>et al.</i> (2009)
Boidae	<i>Boa constrictor</i>	AB177354	Dong and Kumazawa (2015)
Cylindrophidae	<i>Cylindrophis ruffus</i>	AB179619	Dong and Kumazawa (2015)
Xenopeltidae	<i>Xenopeltis unicolor</i>	AB179620	Dong and Kumazawa (2015)
Pythonidae	<i>Python regius</i>	AB177878	Dong and Kumazawa (2015)

References

- Castoe T. A., de Koning A. P. J., Kim H. M., Gu W., Noonan B. P., Naylor G., Jiang Z., Parkinson C. L., Pollock D. D. 2009. Evidence for an ancient adaptive episode of convergent molecular evolution. *Proc Natl Acad Sci USA*, 106(22): 8986–8991
- Chen N., Zhao S. 2009. New progress in snake mitochondrial gene rearrangement. *Mitochondrial DNA*, 20(4): 69–71
- Dong S., Kumazawa Y. 2005. Complete mitochondrial DNA sequences of six snakes: phylogenetic relationships and molecular evolution of genomic features. *J Mol Evol*, 61(1): 12–22
- Douglas D. A., Jank A., Arnason U. 2006. A mitogenomic study on the phylogenetic position of snakes. *Zool Scr*, 35(6): 545–558
- Hall J. B., Cobb V. A., Cahoon A. B. 2013. The complete mitochondrial DNA sequence of *Crotalus horridus* (timber rattlesnake). *Mitochondrial DNA*, 24(2): 94–96
- Han X., Zhao S., Xu C. 2015. Sequence and organization of the complete mitochondrial genome of the *Ussuri mamushi* (*Gloydius ussuriensis*). *Mitochondrial DNA A*, 27: 2617–2618
- He M., Feng J., Zhao E. 2010. The complete mitochondrial genome of the Sichuan hot-spring keel-back (*Thermophis zhaoermii*; Serpentes: Colubridae) and a mitogenomic phylogeny of the snakes. *Mitochondrial DNA*, 21(1): 8–18
- Huang X., Zhang L., Pan T., Zhang B. 2014. Mitochondrial genome of *Protobothrops dabieshanensis* (Squamata: Viperidae: Crotalinae). *Mitochondrial DNA*, 25(5): 337–338
- Jang K. H., Hwang U. W. 2011. Complete mitochondrial genome of the black-headed snake *Sibynophis collaris* (Squamata, Serpentes, Colubridae). *Mitochondrial DNA*, 22(4): 77–79
- Jiang Z. J., Castoe T. A., Austin C. C., Burbrink F. T., Herron M. D., McGuire J. A., Parkinson C. L., Pollock D. D. 2007. Comparative mitochondrial genomics of snakes: extraordinary substitution rate dynamics and functionality of the duplicate control region, *BMC Evol Biol*, 7: 123
- Li E., Feng D., Yan P., Xue H., Chen J., Wu X. 2014. The complete mitochondrial genome of *Oocatochus rufodorsatus* (Reptilia, Serpentes, Colubridae). *Mitochondrial DNA*, 25(6): 449–450
- Li E., Sun F., Zhang R., Chen J., Wu X. 2016. The complete mitochondrial genome of the striped-tailed rat-snake, *Orthriophis taeniurus* (Reptilia, Serpentes, Colubridae). *Mitochondrial DNA*, 27(1): 599–600
- Liu P., Zhao W. 2015. The complete mitochondrial genome of the Amur rat-snake *Elaphe schrenckii* (Squamata: Colubridae). *Mitochondrial DNA A*, 27(4): 2529–2530
- Liu P., Zhao W. 2016. Sequencing and analysis of the complete mitochondrial genome of *Elaphe anomala* (Squamata: Colubridae). *Mitochondrial DNA A*, 27(6): 2742–2743
- Mulcahy D. G., Macey J. R. 2009. Vicariance and dispersal form a ring distribution in nightsnakes around the Gulf of California. *Mol Phylogenet Evol*, 53(2): 537–546
- Mulcahy D. G., Marúnez-Gómez J. E., Aguirre-León G., Cervantes-Pasqualli J. A., Zug G. R. 2014. Rediscovery of an endemic vertebrate from the remote Islas Revillagigedo in the Eastern Pacific Ocean: the Clarión nightsnake lost and found. *PLoS ONE*, 9(5): e97682
- Oh D. J., Han S. H., Kim B. S., Yang K. S., Kim T. W., Koo K. S., Chang M. H., Oh H. S., Jung Y. H. 2015. Mitochondrial genome sequence of *Sibynophis chinensis* (Squamata, Colubridae). *Mitochondrial DNA*, 26(2): 315–316
- Qian L., Wang H., Yan J., Pan T., Jiang S., Rao D., Zhang B. 2018. Multiple independent structural dynamic events in the evolution of snake mitochondrial genomes. *BMC Genomics*, 19: 354
- Singchat W., Areesirisuk P., Sillapaprayoon S., Muangmai N., Srikulnath K. 2019. Complete mitochondrial genome of Siamese cobra (*Naja kaouthia*) determined using next-generation sequencing. *Mitochondrial DNA B*, 4(1): 577–578
- Song T., Zhang C., Zhang L., Huang X., Hu C., Xue C., Zhang B. 2015. Complete mitochondrial genome of *Trimeresurus albolabris* (Squamata: Viperidae: Crotalinae). *Mitochondrial DNA*, 26(2): 291–292
- Sun F. H. 2017. Revealing the complete mitochondrial genome of *Thermophis baileyi* Wall, 1907 (Reptilia: Colubridae) through the next-generation sequencing. *Mitochondrial DNA B*, 2(2): 391–392

- Sun H., Li E., Sun L., Yan P., Xue H., Zhang F., Wu X. 2017. The complete mitochondrial genome of the greater green snake *Cyclophiops major* (Reptilia, Serpentes, Colubridae). Mitochondrial DNA B, 2(1): 309–310
- Wan R., Liu S., Xu Q., Yue B., Zhang X. 2016. The complete mitochondrial genome of the *Elaphe perlacea* (Squamata: Colubridae). Mitochondrial DNA, 27(1): 12–13
- Wang X. H. 2014. Systematics of *Oligodon ningshaanensis* Yuan, 1983 and primary study on its malacophagous behaviour. Doctoral Dissertation, Chengdu Institute of Biology, Chinese Academy of Sciences (In Chinese with English abstract)
- Xu C., Mu Y., Kong Q., Xie G., Guo Z., Zhao S. 2016a. Sequencing and analysis of the complete mitochondrial genome of *Elaphe davidi* (Squamata: Colubridae). Mitochondrial DNA A, 27(4): 2383–2384
- Xu C., Xie F., Liu Y., Zhao S., Wang Y., Ma T., Zhao T. 2015a. Sequencing and analysis of the complete mitochondrial genome of *Gloydus saxatilis* (Squamata: Viperidae: Crotalinae). Mitochondrial DNA A, 27(4): 2361–2362
- Xu C., Zhao S., Han X. 2016b. Sequence and organization of the complete mitochondrial genome of *Hebius vibakari ruthveni* from China. Mitochondrial DNA A, 27(4): 2661–2662
- Xu C., Zhao S., Li C., Dou H. 2015b. The complete mitochondrial genome of *Gloydus intermedius* (Squamata: Viperidae: Crotalinae) from China. Mitochondrial DNA, 27(4): 2373–2374
- Yan J., Li H., Zhou K. 2008. Evolution of the mitochondrial genome in snakes: Gene rearrangements and phylogenetic relationships. BMC Genomics, 9: 569–569
- Yan L., Geng Z., Yan P., Wu X. 2016. The complete mitochondrial genome of *Elaphe bimaculata* (Reptilia, Serpentes, Colubridae). Mitochondrial DNA A, 27(2): 1285–1286
- Zhou B., Ding C., Duan Y., Hui G. 2016. The complete mitochondrial genome sequence of *Ptyas mucosus*. Mitochondrial DNA B, 1(1): 193–194

Table S3 Best-fit models and partitioning schemes selected by PartitionFinder 2.

Subset	Best model	Partition identity
P1	GTR+I+G	ND5_1st, ND4L_1st, ATP6_1st, ATP6_2nd, ND4L_3rd, ATP6_3rd, ATP8_3rd, tRNA_Leu1, COX1_1st, COX1_2nd, ATP8_2nd, ND4_3rd, ND3_3rd COX2_3rd, COX3_2nd, COX3_3rd, tRNA_Lys, Cytb_1st, ND4_2nd, Cytb_2nd, tRNA_Ile, tRNA_Ser1, tRNA_Thr, ND1_1st, ND1_2nd, ND1_3rd ND2_1st, ND2_2nd, ND2_3rd, ND3_1st, ND6_1st, ND6_2nd, ND6_3rd, 16S rRNA, tRNA_Phe, 12S rRNA, tRNA_Val, tRNA_Ser2, tRNA_Gln, COX2_1st, ND5_2nd, COX3_1st, Cytb_3rd, ND4L_2nd, COX1_3rd, ND3_2nd, ND4_1st
P2	GTR+G	ATP8_1st, ND5_3rd, tRNA_Trp, tRNA_Leu2, tRNA_Met, tRNA_Alal, tRNA_Asn, tRNA_Asp, tRNA_Glu, tRNA_Gly, tRNA_His, tRNA_Arg, tRNA_Pro
P3	HKY+I+G	COX2_2nd
P4	SYM+G	tRNA_Tyr, tRNA_Cys

Table S4 Structure traits of the mitochondrial DNA complete control region (D-loop, CR) in *Psammophis lineolatus* and seven snake species of the family Elapidae.

(a) *Psammophis lineolatus*

Unit	Position		Length (bp)	5'–3' motif sequence
	From	To		
CR II	3560	4571	1012	
C-rich	3601	3620	20	CCCCCCCCCTACCCCCCCC
TAS1	3676	3685	10	ACATTAATGG
TAS2	3717	3726	10	ATAATAATTA
CSB III	3864	3877	14	AAATCCTCTATCCT
CSB I	4220	4242	23	TTCCTTAATGCTTGGTAGACATA
CR I	16 145	17 166	1022	
C-rich	16 191	16 210	20	CCCCCCCCCTACCCCCCCC
TAS1	16 266	16 275	10	ACATTAATGG
TAS2	116 307	16 316	10	ATAATAATTA
CSB III	16 454	16 467	14	AAATCCTCTATCCT
CSB I	16 813	16 835	23	TTCCTTAATGCTTGGTAGACATA

(b) *Naja naja*

Unit	Position		Length (bp)	5'–3' motif sequence
	From	To		
CR II	3587	4614	1028	
C-rich	3610	3627	18	CCCCCCCCCTCCCCCCCC
TAS1	3699	3709	11	ACATTAATGAT
CSB III	3886	3899	14	AAATCCTCTATCCT
CSB I	4241	4264	23	TTCCTCCATGATTATAAGACATAT
TAS2	4400	4410	11	AATATAATTAT
CSB II	4537	4550	14	AATCCCCCCGACAC
CR I	16 185	17 213	1029	
C-rich	16 205	16 222	18	CCCCCCCCCTCCCCCCCC
TAS1	16 294	16 304	11	ACATTAATGAT
CSB III	16 481	16 494	14	AAATCCTCTATCCT
CSB I	16 836	16 859	23	TTCCTCCATGATTATAAGACATAT
TAS2	16 995	17 005	11	AATATAATTAT
CSB II	17 132	17 145	14	AATCCCCCCGACAC

(c) *Naja kaouthia*

Unit	Position		Length (bp)	5'–3' motif sequence
	From	To		
CR II	3581	4608	1028	
C-rich	3604	3621	18	CCCCCCCCCTCCCCCCCC
TAS1	3693	3703	11	ACATTAATGAT
CSB III	3880	3894	14	AAATCCTCTATCCT
CSB I	4236	4259	23	TTCCTCCATGATTATAAGACATAT
TAS2	4395	4405	11	AATATAATTAT
CSB II	4531	4544	14	AATCCCCCCGACAC
CR I	16 177	17 203	1027	
C-rich	16 195	16 212	18	CCCCCCCCCTCCCCCCCC
TAS1	16 284	16 294	11	ACATTAATGAT
CSB III	16 472	16 485	14	AAATCCTCTATCCT
CSB I	16 827	16 850	23	TTCCTCCATGATTATAAGACATAT
TAS2	16 986	16 996	11	AATATAATTAT
CSB II	17 123	17 136	14	AATCCCCCCGACAC

Continued Table S4

(d) *Naja atra*

Unit	Position		Length (bp)	5'–3' motif sequence
	From	To		
CR II	3587	4615	1029	
C-rich	3610	3628	19	CCCCCCCCCTCCCCCCCC
TAS1	3700	3710	11	ACATTAATGAT
CSB III	3887	3900	14	AAATCCTCTATCCT
CSB I	4242	4265	23	TTCCTCCATGATTATAAGACATAT
TAS2	4401	4411	11	AATATAATTAT
CSB II	4538	4551	14	AATCCCCCGACAC
CR I	16 186	17 216	1031	
C-rich	16 206	16 225	20	CCCCCCCCCCCCCTCCCCCCC
TAS1	16 297	16 307	11	ACATTAATGAT
CSB III	16 484	16 497	14	AAATCCTCTATCCT
CSB I	16 839	16 862	23	TTCCTCCATGATTATAAGACATAT
TAS2	16 998	17 008	11	AATATAATTAT
CSB II	17 135	17 148	14	AATCCCCCGACAC

(e) *Ophiophagus hannah*

Unit	Position		Length (bp)	5'–3' motif sequence
	From	To		
CR II	3572	4589	1018	
C-rich	3594	3613	20	CCCCCCCCCTACCCCCCCCC
TAS1	3686	3696	11	ACATTAATGAT
TAS2	3726	3736	11	ACTATAATTAT
CSB III	3873	3886	14	AAACCCTCTATCCT
CSB I	4228	4250	23	TTCTTCCATGCTCGTTAGACATA
CSB II	4416	4429	14	ACACCCCCTGACAC
CR I	16 260	17 267	1008	
C-rich	16 281	16 300	20	CCCCCCCCCTACACCCCCC
TAS1	16 373	16 383	11	ACATTAATGAT
TAS2	16 413	16 423	11	ACTATAATTAT
CSB III	16 560	16 573	14	AAACCCTCTATCCT
CSB I	16 915	16 937	23	TTCTTCCATGCTCGTTAGACATA
CSB II	17 103	17 116	14	ACACCCCCTGACAC

(f) *Micrurus fulvius*

Unit	Position		Length (bp)	5'–3' motif sequence
	From	To		
CR II	3551	4705	1155	
C-rich	3575	3591	17	CCCCCCCCCTCCCCCCC
TAS1	3664	3674	11	ACATTAATGTT
CSB III	3851	3864	14	AAACCCTCTATCCT
CSB I	4205	4227	23	TTCCTTCATGCTTGGTAGACATA
TAS2	4586	4596	11	ATAAAAATTAT
CR I	16 312	17 506	1195	
C-rich	16 335	16 352	18	CCCCCCCCCTCCCCCCCC
TAS1	16 425	16 435	11	ACATTAATGTT
CSB III	16 612	16 625	14	AAACCCTCTATCCT
CSB I	16 966	16 988	23	TTCCTTCATGCTTGGTAGACATA
TAS2	17 374	17 357	11	ATAAAAATTAT

Continued Table S4

(g) *Bungarus multioinctus*

Unit	Position		Length (bp)	5'-3' motif sequence
	From	To		
CR II	3555	4568	1014	
C-rich	3576	3597	22	CCCCCCCCCTACCCCCCGCC
TAS1	3666	3676	11	ACATTAATCTA
CSB III	3855	3868	14	AAACCCTCTATCCT
CSB I	4210	4232	23	TTCCTTCATGCTTGTTAGACATA
TAS2	4345	4355	11	ATAATAAACT
CR I	16 104	17 144	1041	
C-rich	16 125	16 148	24	CCCCCCCCCTACCCCCCGCC
TAS1	16 217	16 227	11	ACATTAATCTA
CSB III	16 406	16 419	14	AAACCCTCTATCCT
CSB I	16 761	16 783	23	TTCCTTCATGCTTGTTAGACATA
TAS2	16 896	16 906	11	ATAATAAACT

(h) *Bungarus fasciatus*

Unit	Position		Length (bp)	5'-3' motif sequence
	From	To		
CR II	3563	4580	1018	
C-rich	3585	3604	20	CCCCCCCCCTCCCCCCCC
TAS1	3677	3687	11	ACATTAATGTT
CSB III	3865	3878	14	AAACCCTCTATCCT
CSB I	4220	4242	23	TTCCTTCATGCTTGTTAGACATA
TAS2	4278	4288	11	ATAGTAATTTT
CR I	16 138	17 234	1097	
C-rich	16 160	16 180	21	CCCCCCCCCTCCCCCCCC
TAS1	16 253	16 263	11	ACATTAATGTT
CSB III	16 441	16 454	14	AAACCCTCTATCCT
CSB I	16 796	16 818	23	TTCCTTCATGCTTGTTAGACATA
TAS2	16 854	16 864	11	ATAGTAATTTT